FRACTURE GEOMETRY AND RELATIVE PERMEABILITIES: APPLICATION TO MULTIPHASE FLOW THROUGH COAL

J. P. Morris, Purdue University
L. J. Pyrak-Nolte, Purdue University
N. J. Giordano, Purdue University
Jiangtao Cheng, Purdue University
John Tran, University of Notre Dame
Andrew Lumsdaine, University of Notre Dame

ABSTRACT

A numerical investigation of the multiphase flow properties of coal was performed to identify possible relationships among fracture network geometry, relative permeability, and absolute permeability. A stratified percolation algorithm was used to generate individual fractures with spatially correlated and uncorrelated aperture distributions. These fractures were arranged on a cubic lattice to produce a network of intersecting fractures to approximate coal cleats. The relative permeabilities of the resultant fracture network were determined using an efficient network flow model. Statistical flow properties of the fracture networks were obtained by examining the results of a number of realizations from each fracture network configuration. No simple relationship between relative permeability and the bulk properties of the coal cleat network was found. However, in general, networks of uncorrelated fractures were observed to have lower non-wetting saturations at cross-over than correlated fractures. Simulated fracture networks containing fractures with a range of average apertures were observed to most closely approximate experimentally determined values of relative permeability of coal cores. These results indicate that an estimate of the variation in average fracture aperture may provide indications of relative permeability behavior.

INTRODUCTION

The potential methane yield from a coalbed reservoir depends upon many competing factors. For example, high water production rates can be an economic barrier to gas resource exploitation. Natural fractures (cleats) are the conduits for fluid transport within these reservoirs. Accurate gas-water relative permeability data for coal cleats are crucial for reliably assessing the development potential of these gas reservoirs. Three methods can be used to determine this critical reservoir property: (1) wellbore pressure transient testing; (2) laboratory drill core testing; and (3) theoretical three-dimensional (3-D) multiphase flow simulation modeling. Unfortunately, wellbore test data do not provide a unique determination of permeability properties, and laboratory test methods lack accuracy and precision [1]. Controlled three-dimensional numerical studies of multiphase flow through fracture networks provide an alternative method for determining the relationship between relative permeability and fracture network geometry. While numerical simulations offer precise estimates of flow properties, many computational techniques require detailed knowledge of the aperture distribution within each fracture and the precise locations of intersections within the fracture network.

This paper presents relative permeability saturation behavior obtained using a network model optimized for solution of flow through interconnected fractures. The method is sufficiently fast that large numbers of fracture network realizations can be simulated and population statistics performed. In this way, insight into the effects of macroscopic geometrical properties (fracture density, fracture orientation, number of fracture sets) for a large number of realizations with chosen characteristics can be investigated. Both averaged values and confidence intervals based on Monte Carlo simulation, are readily generated for absolute permeability, the capillary pressure - saturation relationship, and relative permeability.

Single phase flow through fracture networks has been studied extensively for both two- and three-dimensional representations of fracture networks assuming a constant aperture within each fracture. For

example, Long and Witherspoon[2] investigated the relationship between fracture interconnectivity and network permeability using a two-dimensional model. Three-dimensional networks have been modeled using arrangements of disk shaped discontinuities[3]. Tsang et al.[4] employed a system of one-dimensional channels to model transport through the preferred flow paths of a fractured medium. Nordqvist et al.[5] employed a three-dimensional variable-aperture fracture network model to investigate the relationship between fracture transmissivity and tracer transport. Their method integrated results from a library of single fracture permeabilities to estimate the properties of the three-dimensional network. Nordqvist et al.[5] found that the transport properties of the network depended strongly upon the variability of the fracture transmissivity. Relatively little work has been done investigating the relative permeability of fully three-dimensional fracture networks containing realistic aperture distributions within each fracture. Our technique is built around a versatile fracture description language which allows families of fractures to be designated in terms of their statistical attributes.

NUMERICAL GENERATION OF FRACTURE GEOMETRY

Numerically generated fractures were used to explore the effect of the size and spatial distributions of apertures in the two-dimensional fractures on the relative permeability of a three-dimensional fracture network. Simulated fractures were generated with both correlated (long-range) and uncorrelated (short-range) spatial aperture distributions. Each fracture was represented by a 300 by 300 array of apertures where each element of the array represents a single aperture. These fractures were inserted into a cubic lattice to produce a network of fractures.

Uncorrelated fractures were generated by taking an initially zero aperture fracture and randomly placing small squares (points) of fixed aperture within the array. Figure 1a contains a representative image of a spatially uncorrelated fracture generated using this method. This image represents a fracture with a random distribution of apertures that is spatially uncorrelated i.e., the spatial correlation is on the order of the point size.

The spatially correlated aperture distributions were based on a hierarchical construction of the fracture aperture distribution known as stratified percolation [6, 7, 8]. The stratified percolation method for generating synthetic two-dimensional fractures is performed by a recursive algorithm that defines a self-similar cascade. Classical random continuum percolation is applied on successively smaller scales (tiers). Several (n) randomly positioned, equi-sized squares are chosen within the fracture array (the first tier). Within each sub-square (the second tier), n smaller squares are chosen. The sub-squares are reduced in linear size by a constant scale factor from the previous tier square size. This recursive process is continued until the final tier is reached. At this stage, small squares (points) of fixed aperture are placed at the origin of each sub-square of the final tier. The aperture of the fracture at a given location is taken to be proportional to the number of final points accumulated there. This approach leads to long-range spatial correlations because regions of non-zero aperture can only occur within squares selected on tiers throughout the hierarchy. Figures 1b and c show correlated fractures generated using this method with 5 tiers. Fractures b and c differ only in the initial seed used by the random number generator.

The fractures were placed on a cubic lattice to produce a fracture network resembling that of coal cleats. For example, Figure 2a shows a cubic volume containing three fractures (two perpendicular to the *x*-axis and one perpendicular to the *y*-axis). If the network is generated a second time with different seed values, a substantially different aperture network is produced (Figure 2b).

COMPUTATIONAL FLOW MODEL

The multiphase flow properties of the void space generated by the system of intersecting fractures was investigated using a network model. Network methods have been used extensively to study both single and multiphase flow through two- and three-dimensional pore-spaces (see [9] for a review). One attraction of network models is that they approximate fluid behavior at the pore scale, rather than assuming field-scale constitutive relationships. Network flow models are fast and are flexible, and can accommodate progressively more complicated fluid properties.

Though originally used for single phase flow, the flexible nature of the network permits extensions to include multicomponent behavior. Quasi-static network models, for example, have been successfully ap-

plied to multiphase problems. These methods assume a set of rules which determine the movement of the fluids and fluid-fluid interfaces through the pore network. For example, for a meniscus to enter a pore throat, it must overcome the capillary pressure acting against this motion. Rules accounting for wetting films, hysteresis, trapping of fluids, and gravity have also be developed[10].

In this study, we have investigated networks of fractures featuring realistic aperture distributions within each fracture, and explored the statistical variations in flow properties between individual realizations of fracture networks. Global accessibility rules were used to determine those portions of the network accessible to each fluid phase. The algorithm considers the range of aperture values in discrete steps. At each level, all fracture sites with apertures smaller than the current level are assumed to be saturated by the wetting fluid. All other sites are saturated with the non-wetting fluid (Figure 3a,b). Networks (Figure 3c) are then generated for each available void space and permeabilities are calculated. The network model used to approximate the void space is similar to that of Yang et al.[11] and Tran[12]. This method replaces the fracture with a network of elliptical cross-section pipes to approximate the flow properties of the fracture. The algorithm for generating the network of pipes proceeds from the inlet side of the fracture to the outlet side. Using the algorithm of Yang et al.[11] and Tran[12] each row of pixels perpendicular to the global flow direction is considered in turn. Regions of non-zero aperture are approximated by single large flow elements of elliptical cross-section (Figure 4). The flow elements generated in neighboring rows are linked by pipes with conductances given by the analytic solution for flow through an elliptical cross-section pipe[13].

The algorithm used by Tran[12] generates pipes which link the mid-point of elements in neighboring rows. This method was found to induce unphysical flow rates for some applications[14]. In this work, flow elements in neighboring rows were joined by pipes of the maximum width such that they fitted within the neighboring flow elements. In addition, it was found that by coalescing entire contiguous regions of non-zero aperture in each row, the flow rate was over estimated. Typical flow simulations may involve regions where flow proceeds from a narrow region into a wider region. Although flow streamlines result in some areas being effectively inaccessible, the algorithm discussed above creates a single flow element which includes these regions and, consequently, flow is overestimated. To avoid this, flow elements in adjacent rows were not allowed to produce flow paths which diverge by more than 45°. This corresponds to assuming that the local flow is predominantly in the same direction as the global flow. Figure 3c shows an example of a network generated to approximate the volume available to the non-wetting phase (Figure 3b). For fractures oriented perpendicular to the flow direction, these directional approximations are inappropriate. Where no global flow direction could be identified, a network was generated using a parallel plate approximation for flow into and out of each pixel of the fracture.

The resultant method has been found to agree very closely with experimental data and alternative network generation techniques[14]. For example, Figure 5 shows a comparison between results obtained using the elliptical pipe algorithm and experimental measurement of the absolute permeability of spatially correlated micromodels. Implicit in the network generation method is the assumption that the fluid flow is laminar and well approximated by the analytic solutions employed locally.

RESULTS

For a given set of parameters, the fracture generation algorithms discussed will produce fractures with potentially different flow properties (e.g. see Figure 1b and c). In the laboratory it is difficult to consider the flow properties of more than a small number of fracture networks. The speed of modern computers makes it possible to calculate the flow properties of many realizations of statistically similar fracture networks and to study variations over a larger population of samples.

This paper presents a summary of results obtained as part of an extensive study of multiphase flow through three-dimensional fracture networks. The results presented are for the flow of methane (non-wetting fluid) and water (wetting fluid) caused by an applied pressure gradient parallel to the z-axis of a cube measuring 0.1m on a side (Figure 2a). The fluid properties are in Table 2. The relationship between the various properties of the fracture network and relative permeability of the fracture network was investigated by varying both the individual properties of the fractures and the geometry of the fracture network. We have considered several different types of fracture with both spatially uncorrelated and correlated apertures (the precise fracture geometry specifications are in Table 1).

The relative permeability of single uncorrelated and correlated fractures is shown as a function of non-

wetting saturation (gas saturation) in Figure 6. The error bars on the simulated data correspond to 20% of the standard deviation away from the mean, based upon a sample of 50 realizations. Because the spatially uncorrelated fractures have a random spatial aperture distribution, the variations in relative permeability are relatively small for different realizations. However, spatially correlated fractures exhibit more variation in relative permeability because the spatial aperture distribution varies widely among realizations.

Single fractures generated using the parameters in Table 1 will not reproduce the experimental results (Figure 7) To further explore the relationship between fracture network geometry and flow properties, successively more complicated fracture networks were studied. We have devised networks of multiple intersecting fractures which closely match the experimental results (Figure 7). The properties of these fracture networks will be explored in the following sections.

With a view to obtaining a better fit to the experimental data, three successive levels of complexity were introduced to the fracture network realizations to study the effect of fracture network geometry on relative permeability:

1. Increasing the number of statistically similar fractures.

2. Enlarging the spatial dimensions of the intersections.

3. Varying the relative void volume among fractures in the network.

Increasing the number of similar fractures

As the number of fractures in a fracture network is increased, the number of fracture intersections also increases. This was found to only significantly effect the relative permeability if the aperture distributions were correlated. The spatial correlations of the correlated fractures produce relatively few large aperture, connected flow paths. The probability that these flow paths will span the cube increases as the number of fractures is increased. Consequently, the non-wetting phase saturation at cross-over, S_X, (see Figure 7 for definition) is reduced by up to 15% for networks with correlated aperture distributions as the number of intersections is increased (Figure 8a).

The relative permeability at cross-over (K_X) exhibited a slight increase with the number of intersections for correlated fractures (Figure 8b) The average K_X was substantially lower for the uncorrelated fractures because all uncorrelated fractures in the network have very similar flow properties and individually do not support the flow of both phases at any given saturation (Figure 6).

Enlarging the intersections

In real fracture networks, the intersections of the fracture planes may become enlarged through chemical or mechanical erosion or other processes. We simulated these enlarged flow paths by increasing the apertures along lines of intersection.

The enlarged intersections lead to enhanced non-wetting flow along intersections parallel to the flow direction (z-axis) regardless of the correlations in the aperture distributions. The saturation at cross-over was observed to decrease by approximately 15% as more fractures were introduced to the network (Figure 9a).

Fracture intersections perpendicular to the flow direction (denoted "z-fractures") acted as partial barriers to wetting flow in the uncorrelated fractures. This resulted in lower saturation at cross-over and reduced relative permeability at cross-over (Figure 9b) for networks of uncorrelated fractures.

Varying the relative void volume of multiple fractures

Fracture networks found in natural systems often contain fractures with different average aperture (see, for example, the image of Core D, Figure 10). The wetting fluid preferentially saturates the narrow, less permeable fractures, leading to reduced wetting flow. To simulate this numerically, the apertures of the fractures were rescaled by different factors before being added to the cube

$$\text{new aperture} = \mathcal{C} \times \text{aperture}$$

At least one fracture in the network was left with its original aperture scaling to provide a preferential non-wetting flow path. The average of the re-scaling factors provides an indication of the proportion of the void volume taken up by narrow aperture fractures.

$$B^* = \frac{\sum C_i}{n}$$

A value of B^* approaching 1 indicates most of the network consists of fractures of the same, original average aperture. Smaller values of B^* indicate that more fractures are rescaled to have reduced average apertures. The addition of fractures with variable average aperture led to a reduction in the saturation at cross-over for networks of uncorrelated and correlated fractures without enlarged intersections (Figure 11a). In addition the relative permeability at cross-over remained high (Figure 11b). Figure 7 shows the average relative permeability of 30 realizations of networks containing 12 fractures with $B^* = 0.583$. The average results for the network of uncorrelated fractures is in close agreement with the experimental data for Core A.

CONCLUSIONS

The fracture network generator and network flow model solver are sufficiently fast to investigate the properties of many realizations of a wide range of fracture networks with realistic spatial aperture distributions within the individual fractures. These simulations provide a database of results against which fracture-flow relationships can be tested. The data do not indicate any straight-forward relationships between relative permeability and easily measured bulk properties (porosity, absolute permeability). However, it is possible to make some more general statements regarding the relationship between fracture network geometry and multiphase flow properties.

The correlated fractures supported fewer wide aperture paths (non-wetting flow channels) which did not necessarily span the flow cube. Consequently, networks of uncorrelated fractures were observed to have lower non-wetting saturations at cross-over. The addition of fractures to the network enhanced non-wetting flow for the correlated fracture networks by increasing the probability of connected, wide aperture flow paths. However, the value of relative permeability at cross-over was unphysically small for networks of uncorrelated fractures of the same average aperture because the fractures in the network switch from supporting wetting flow to non-wetting flow at approximately the same level of saturation.

Enlarging fracture intersections lead to increased wetting flow for both correlated and uncorrelated fractures. The results of this study suggest that for the class of fractures considered, networks containing multiple fractures of different average aperture provide the best fit to experimental data.

ACKNOWLEDGMENTS

This work was supported by the Gas Research Institute (Contract No. 5095-260-3532). LJPN wishes to thank the National Science Foundation - Young Investigator Award from the Division of Earth Sciences (NSF/94 58373-001) for support of this research.

REFERENCES

1. Pyrak-Nolte, L. J. and B. W. Gash, 1993; "Multiphase flow through cleats in coal - project summary," Quarterly Review of Methane from Coal Seams Technology, V. 11, No. 2, p. 34–38.
2. Long, J. C. S. and P. A. Witherspoon, 1985; "The relationship of the degree of interconnection to permeability in fracture networks," J. Geophys. Res., V. 90, p. 3087–3098.
3. Long, J. C. S., P. Gilmour and P. A. Witherspoon, 1985; "A model for steady flow in random three-dimensional networks of disc-shaped fractures," Water Res. Research, V. 21, p. 1105–1115.
4. Tsang, Y. W., C. F. Tsang, I. Neretnieks and L. Moreno, 1988; "Flow and tracer transport in fractured media: A variable aperture channel model and its properties," Water Res. Research, V. 24, No. 12, p. 2049–2060.
5. Nordqvist, A. W., Y. W. Tsang, C. F. Tsang, B. Dverstorp and J. Andersson, 1996; "Effects of high variance of fracture transmissivity on transport and sorption at different scales in a discrete model for fractured rocks," J. Contaminant Hydrol., V. 22, p. 39–66.
6. Pyrak-Nolte, L. J., N. G. W. Cook and D. D. Nolte, 1988; "Fluid percolation through single fractures,"

Geophys. Res. Lett., V. 15, p. 1247–1250.
7. Nolte, D. D., L. J. Pyrak-Nolte and N. G. W. Cook, 1989; "Fractal geometry of the flow paths in natural fractures and the approach to percolation," Pure and Appl. Geophys., V. 131, p. 111.
8. Nolte, D. D. and L. J. Pyrak-Nolte, 1991; "Stratified continuum percolation - scaling geometry of hierarchical cascades," Phys. Rev. A, V. 44, No. 10, p. 6320–6333.
9. Celia, M. A. and P. C. Reeves, 1995; "Recent advances in pore scale models for multiphase flow," Rev. Geophys. Suppl., 1049–1057.
10. Soll, W. E. and M. A. Celia, 1993; "A modified percolation approach to simulating three-fluid capillary pressure-saturation relationships," Adv. Water Res., V. 16, p. 107–126.
11. Yang, G. M., L. R. Myer, S. R. Brown and N. G. W. Cook, 1995; "Microscopic analysis of macroscopic transport-properties of single natural fractures using graph-theory algorithms," Geophys. Res. Lett., V. 22, No. 11, p. 1429–1432.
12. Tran, J. J., 1998; "Efficient simulation of multiphase flow in three-dimensional fracture networks," Master's thesis, Department of Computer Science and Engineering, Notre Dame, Indiana.
13. Prasuhn, A. L., 1980; *Fundamentals of fluid mechanics* Englewood Cliffs, N.J. : Prentice-Hall.
14. Morris, J. P., J. Cheng, J. Tran, A. Lumsdaine, N. J. Giordano and L. J. Pyrak-Nolte, 1999; "Single phase flow in a fracture: Micro-model experiments and ab-initio simulation," (in preparation).
15. Gash, B. W., 1991; "Measurement of "rock properties" in coal for coalbed methane production," SPE Report 22909, presented at the 66th Annual Technical Conference and Exhibition of the SPE, Dallas, TX, October 6-9.

Table 1: Parameters used by stratified percolation method to generate uncorrelated and correlated fractures.

property	uncorrelated	correlated	correlated 7pt
dimensions	300×300	300×300	300×300
number of tiers	1	5	5
point size	4	4	4
points per tier	10^5	10	7
scale factor	75	2.37	2.37

Table 2: Viscosity of fluids.

	viscosity (kg/m/s)
water	10^{-3}
methane	1.087×10^{-5}

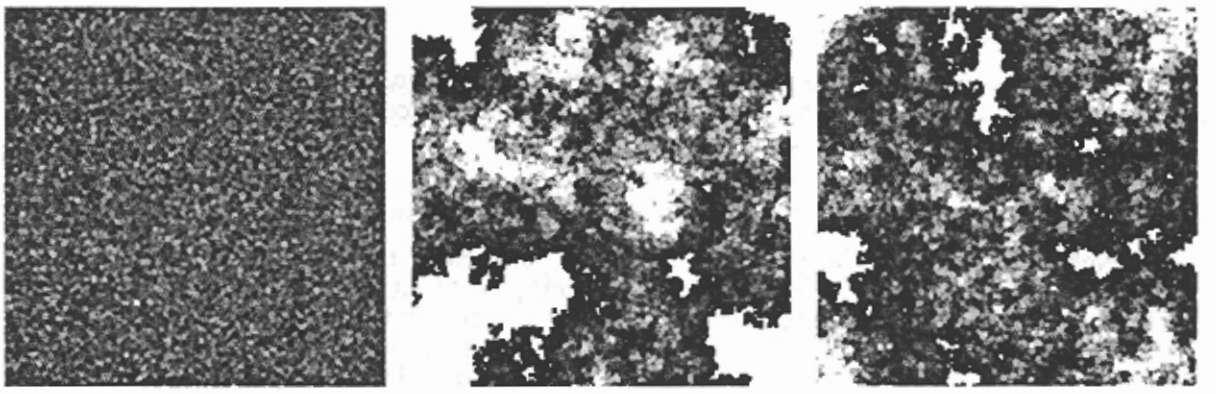

(a) (b) (c)

Figure 1: Fractures with spatially (a) uncorrelated and (b) & (c) correlated aperture distributions. Increasing apertures are shaded from black to light gray with black representing smallest apertures. Regions of contact (zero aperture) are highlighted in white. Fractures (b) and (c) were generated using the stratified percolation algorithm with all parameters identical other than the seed used by the random number generator.

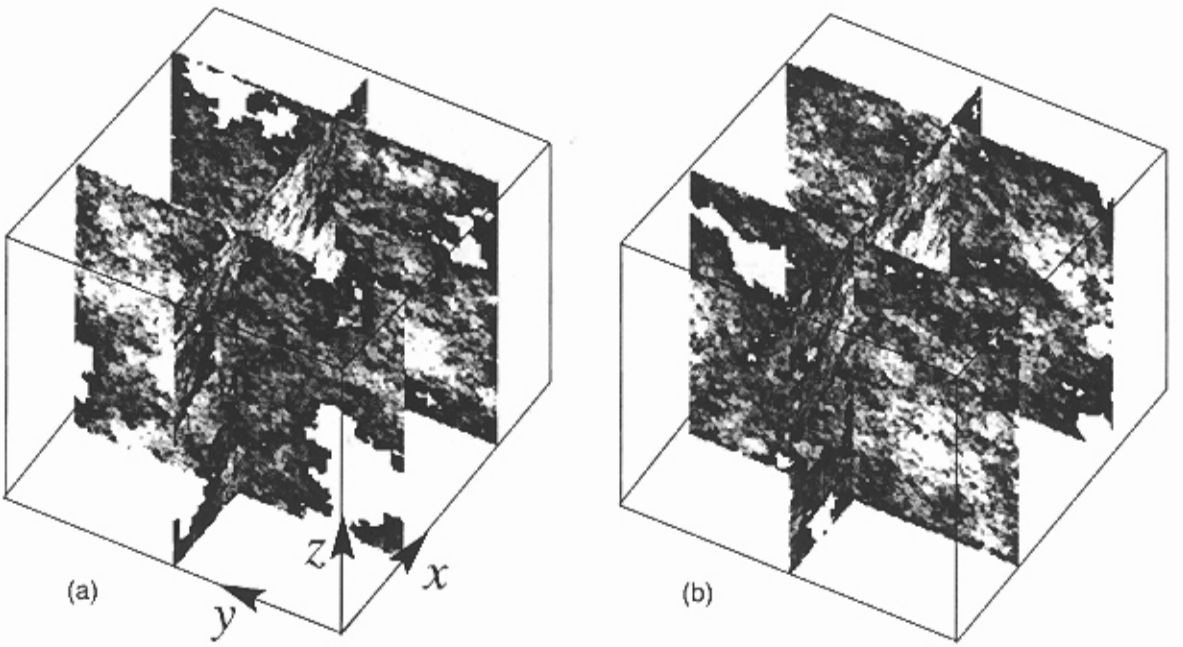

Figure 2: The fractures are placed on a cubic lattice to simulate a fracture network. Different initial seeds will result in potentially very different connectivity between the fractures. These fracture networks were generated using parameters identical other than the initial seed used by the random number generator.

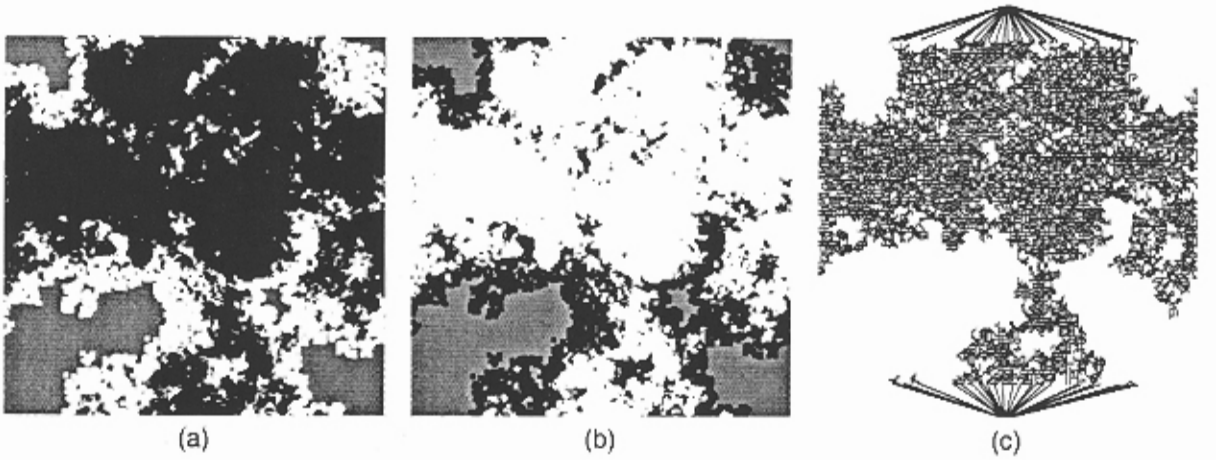

Figure 3: The aperture sites available to (a) wetting fluid and (b) non-wetting fluid are shown in white (contact area is gray, and black is inaccessible). All apertures of the fracture (Figure 1b) smaller than the current level of saturation are occupied by (a) wetting fluid and the rest are occupied by (b) non-wetting fluid. (c) The network of elliptical pipes generated to approximate the non-wetting fluid volume.

Figure 4: Pipes of elliptical cross-section are fitted within the pore-space of each fracture along rows perpendicular to the flow direction.

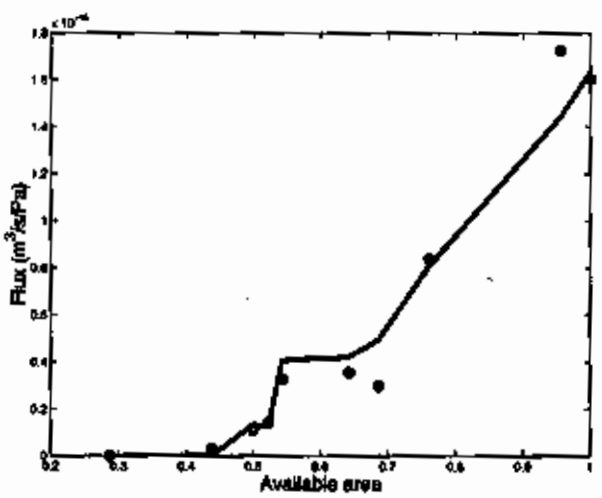

Figure 5: Comparison of numerical results (black curve) with micromodel experiments (circles) [14] for specific realizations of spatially correlated fractures.

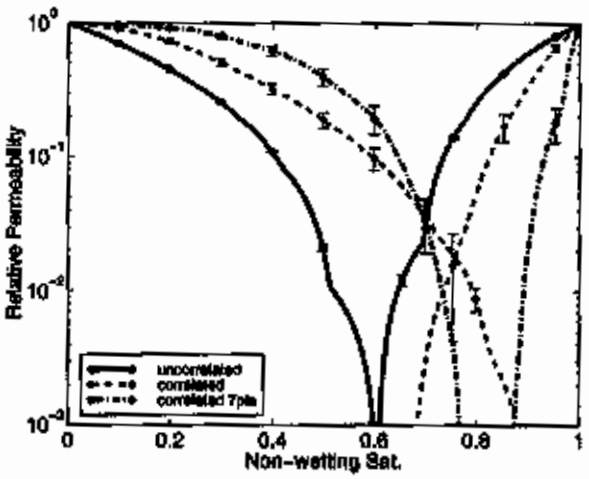

Figure 6: The numerical results for single correlated and uncorrelated fractures. The thick lines are the averages over 50 simulations and the error bars signify 20% of a standard deviation about the mean relative permeability.

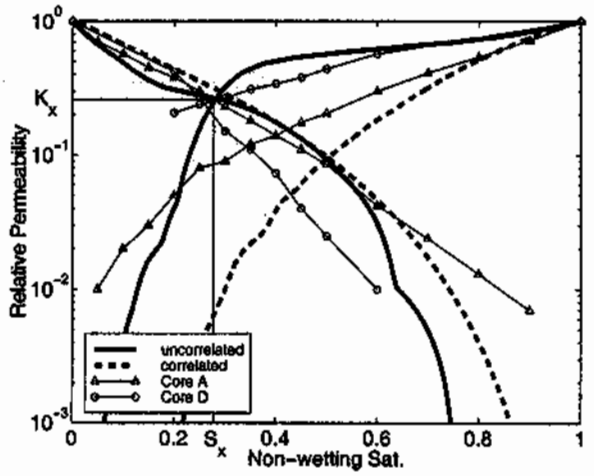

Figure 7: Data obtained for two coal cores[15] and the relative permeability for a network of fractures of differing average aperture (see text for details). S_X is defined to be the non-wetting saturation at the cross-over point and K_X is the value of the relative permeability at that point, i.e., when the wetting and non-wetting relative permeabilities are equal.

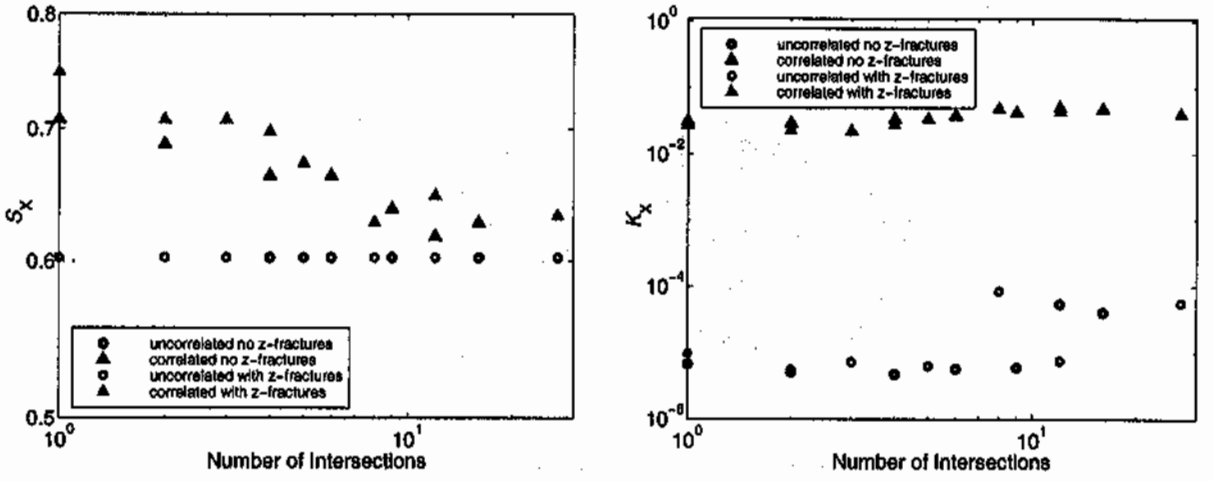

Figure 8: (a) Cross-over saturation and (b) relative permeability at cross-over as number of intersections of statistically similar fractures is increased. S_X only changes significantly for correlated fractures, because more intersections increases the probability that the non-wetting flow spans the cube. The networks of uncorrelated fractures have unphysically low values of K_X.

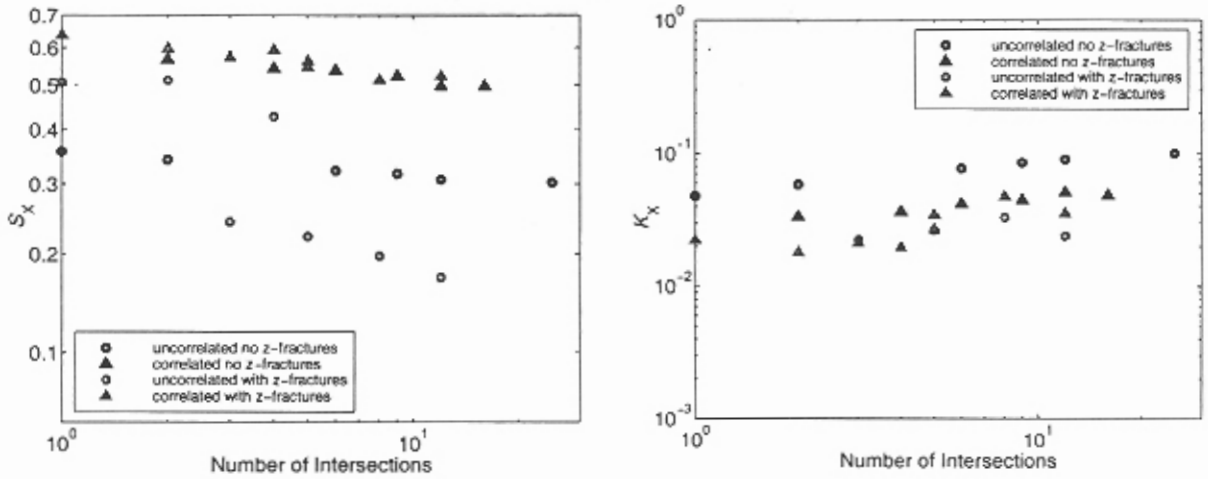

Figure 9: (a) Cross-over saturation and (b) relative permeability at cross-over as number of intersections of statistically similar fractures is increased with enlarged intersections. Both correlated and uncorrelated fractures exhibit a decrease in S_X due to the enlarged intersections. The presence of z-fractures (perpendicular to the flow direction) inhibits wetting flow, leading to lower S_X.

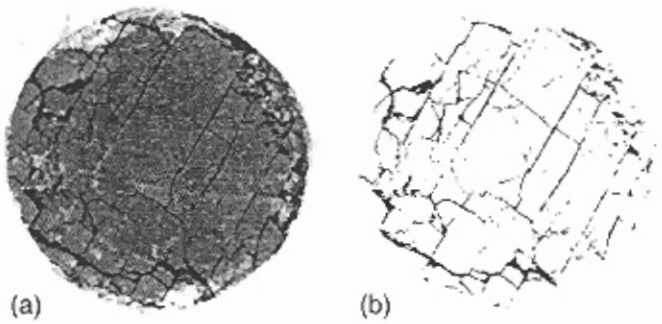

Figure 10: A grayscale image (a) and thresholded image (b) of the end of coal core D of Gash[15]. The sample exhibits fractures with a range of average apertures.

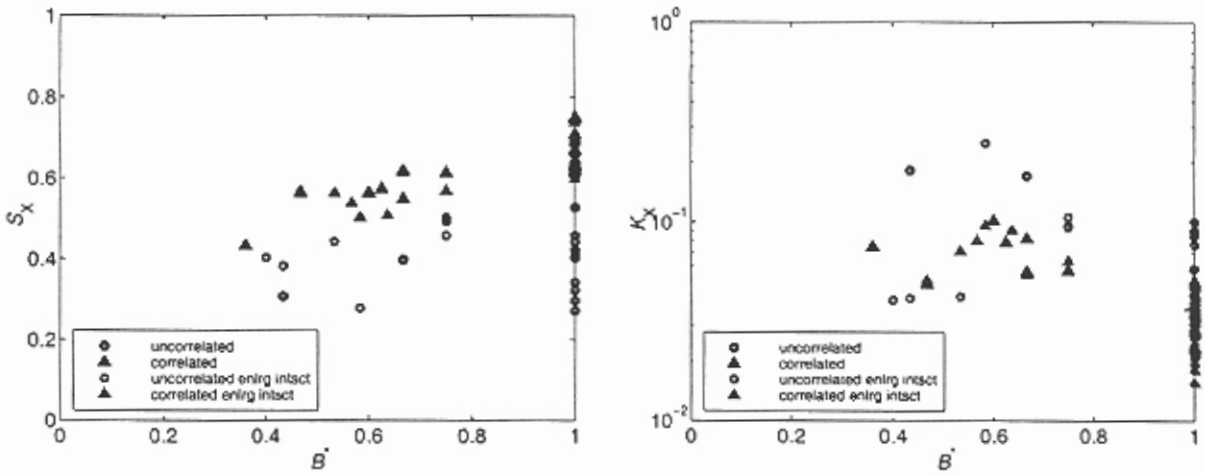

Figure 11: (a) Cross-over saturation and (b) relative permeability at cross-over as a function of the average normalized aperture. Fracture networks containing fractures with a range of average apertures exhibit low S_X and higher K_X. Fracture networks without enlarged intersections show a strong decrease in cross-over saturation as the average normalized aperture decreases.